AIP | Review of Scientific Instruments

Automation for monitoring of the refractive index profile of vapor-phase-deposited soot preforms for optical fiber

J. S. dos Santos, E. Ono, and C. K. Suzuki

Articles you may be interested in

Complete energy transfer due to rare-earth phase segregation in optical fiber preform glasses
J. Appl. Phys. **110**, 083121 (2011); 10.1063/1.3657852

Formation mechanisms of precursors of radiation-induced color centers during fabrication of silica optical fiber preform
J. Appl. Phys. **109**, 083103 (2011); 10.1063/1.3561435

Transient radiation responses of silica-based optical fibers: Influence of modified chemical-vapor deposition process parameters
J. Appl. Phys. **99**, 023104 (2006); 10.1063/1.2161826

Extruded single-mode high-index-core one-dimensional microstructured optical fiber with high index-contrast for highly nonlinear optical devices
Appl. Phys. Lett. **87**, 081110 (2005); 10.1063/1.2034094

Atomic force microscopy for the determination of refractive index profiles of optical fibers and waveguides: A quantitative study
J. Appl. Phys. **82**, 2730 (1997); 10.1063/1.366103

Automation for monitoring of the refractive index profile of vapor-phase-deposited soot preforms for optical fiber

J. S. dos Santos, E. Ono, and C. K. Suzuki
Laboratory of Integrated Quartz Cycle (LIQC), Faculty of Mechanical Engineering, Department of Materials Engineering, State University of Campinas, P.O. Box 6122, 13083-970, Campinas-Sao Paulo, Brazil

The vapor-phase axial deposition process is currently one of the most advantageous methods to produce preforms for optical fibers, due to its high efficiency and reduced production cost. However, this method has great difficulty in determining the refractive index profile, since it is influenced by too many process parameters. In this work, an automation system to determine the refractive index profile by monitoring the preform deposition surface profile during the soot preform deposition stage is presented. Based on a previous study that showed a strong correlation between these two profiles, an automation system was developed in LABVIEW to monitor the deposition surface profile during the preform deposition stage in order to estimate the preform germanium doping profile and refractive index profile, as well as a theoretical study to develop this system in order to minimize the performance impairment. As a result, not only preforms with a predetermined index profile were produced but also a reduction in production cost was obtained by decreasing the number of preform rejects. © *2006 American Institute of Physics.* [DOI: 10.1063/1.2198790]

I. INTRODUCTION

Since optical fiber was developed, it has revolutionized the global communication system. Without the development of low loss silica fiber as a broadband medium for transporting voice, video, and data traffic, worldwide communication would not have been possible. The data carrying capacity of optical fiber is doubling every year as technology advances in photonics and electronics, which permit more and more wavelengths of light to be transmitted at ever increasing data rates.[1]

Optical fiber is produced through the fabrication of the preform and its posterior drawing. After the drawing stage, the optical properties embodied during the preform fabrication remain in the optical fiber. There are many methods to produce optical fiber preforms. Among them, the vapor-phase axial deposition (VAD) method is one of the most advanced due to its high efficiency, high deposition rate, easy processing steps, and reduced production cost.[2]

In the VAD method, nanosize particles of silica (SiO_2) and germania (GeO_2) are synthesized at a high temperature by a hydrolysis and oxidation reaction of metallic halides such as $SiCl_4$ and $GeCl_4$.[3] Germanium is used as a main doping element to increase the refractive index of the fiber core, establishing a refractive index difference between the optical fiber clad and core.[4] For several compositions of binary silica-germania glass prepared by a flame deposition technique, Huang *et al.* have calculated theoretically the refractive index by computing the electronic polarizability of fused silica and germania, and measured empirically the refractive index at the sodium *D* wavelength by the Becke line method using an optical microscope. Both results showed a nearly linear relationship of refractive index with germanium concentration.[5] Fleming has also obtained a nearly linear re-

lationship between the refractive index and germania molar fraction of silica-germania glass by considering the Sellmeier coefficients.[6] Therefore, the radial distribution of germanium concentration defines the refractive index profile. This profile must be accurately controlled since it controls the data transmission characteristics in the optical fiber.

After particle deposition process, the soot preform is submitted to a thermochemical treatment with Cl_2 gas (dehydration) to remove the hydroxyl groups (OH) incorporated into the preform during the deposition. Such impurities cause light attenuation in the region used in optical transmission.[7] After dehydration, the preform is consolidated in a high temperature furnace with a controlled He gas atmosphere and transformed into a transparent and bubble-free preform.

It is difficult to produce preforms with a desired germanium doping profile with high reproducibility and stability in the VAD method, due to the complicated formation mechanism during the soot preform deposition. Many factors, such as H_2/O_2 ratio in the flame, $SiCl_4/GeCl_4$ reactant ratio, burner geometry, radial and axial distributions of deposition temperature, and soot preform geometric shape (diameter and bottom shape), among others, are involved.[8–10] Long-period fluctuations of these parameters cause refractive index profile variations in the axial direction, as several hours are needed to fabricate a long soot preform.

It was reported that there is a strong relationship between refractive index profile and soot preform deposition surface profile, mainly for graded index profiles.[11,12] This relationship was determined through an approximation of the shape of porous preform deposition surface and the corresponding refractive index distribution by an exponential function. For a parabolic refractive index, Chida *et al.* have obtained that the best porous preform deposition surface profile (α) must be about 1.5, while Imoto *et al.* have obtained α
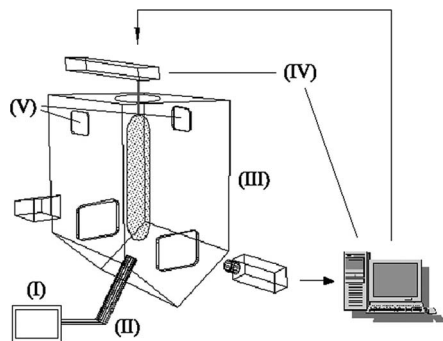
FIG. 1. Schematics of the VAD equipment used to produce soot preforms.

FIG. 2. A five concentric nozzle silica burner.

values in the 2.5–3.0 range. Therefore, by knowing this relationship it is possible to produce preforms with predetermined doping profiles.

In a previous work,[13] a study of the correlation between the germanium doping profile and the deposition surface profile was carried out, and a methodology was presented to estimate the germanium doping profile of VAD preforms through the parametrization of the preform deposition surface profile. Moreover, a sort of deposition parameter to produce VAD preforms with standard and special doping profiles was given.

All these relationships are based on a direct dependence of the effect of preform deposition surface shape on the temperature distribution of the preform deposition surface. Once germania concentration is largely dependent on the deposition surface temperature distribution, the preform deposition surface shape can describe the doping profile and consequently the refractive index profile.[9,13] Furthermore, the refractive index profile is determined not only by the germania concentration but also by the density distribution of porous preform. This one is an important parameter to the shrinkage degree in both radial and axial directions of the preform in the consolidation process. The density profile in the consolidated preform is identical to that of the germanium doping profile in the preform. Therefore, the refractive index profile in the consolidated preform can be estimated from the germania in the porous preform, considering the relationship between the radial densities of the porous preform and the consolidated preform.[14]

The main objective of the present work is to present an automation system developed in LABVIEW in order to monitor the preform deposition surface profile axial uniformity and indirectly estimate the refractive index profile in real time of VAD. This system makes possible, at the beginning of the deposition stage, to establish the doping profile, such as parabolic or triangular gradual profiles, that determines the optical fiber type (for example, multimode or single mode). Moreover, it allows the germanium doping profile to be reproduced and axial uniformity variations of the doping profile to be identified, minimizing preform rejects, so that production cost can be improved.

II. EQUIPMENT FOR VAD PREFORM FABRICATION

The equipment used in this research for the deposition of VAD preforms is represented in Fig. 1. It is basically com-
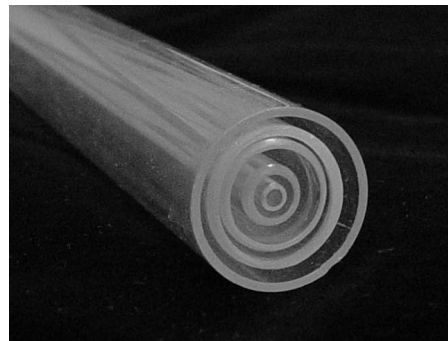
posed of (I) a system for gas supply, (II) burner, (III) deposition chamber, (IV) pulling mechanism and automated position control system of the preform, and (V) exhaust system.

All gases are simultaneously injected into a five concentric nozzle silica burner (Fig. 2). The metallic halides ($GeCl_4$ and $SiCl_4$) are expelled from the central tube, while adjacent tubes expel fuel gases (H_2 and O_2) and inert gases (N_2), used to control the flame temperature and burner protection.

III. PREFORM FABRICATION AND CHARACTERIZATION

For the theoretical study of the automation system, several preforms with dimensions of about 200 mm in length and 40 mm in diameter were deposited (Fig. 3). The burner used for the preform deposition was the five concentric nozzle silica burner and the gas fluxes for H_2, O_2, and $SiCl_4$ were 3600, 5200, and 150 SCCM, respectively (SCCM denotes cubic centimeter per minute at STP). Other experimental conditions were $GeCl_4$ flux in the 40–50 SCCM range, distance of target to burner in the 45–48 mm interval, and 38°–45° setting angle of the burner related to the target.

In the deposition process, in order to control the uniformity of the preform geometry, a feedback automation system
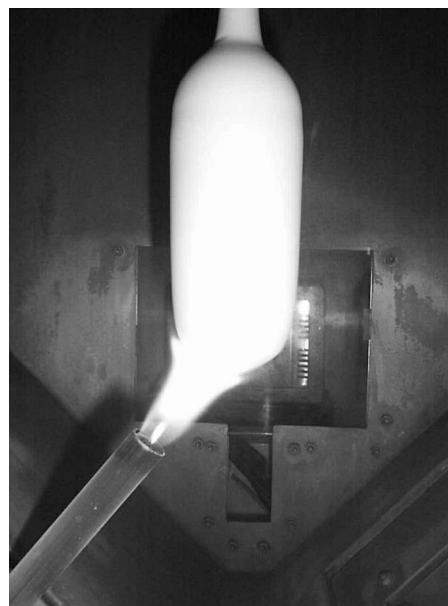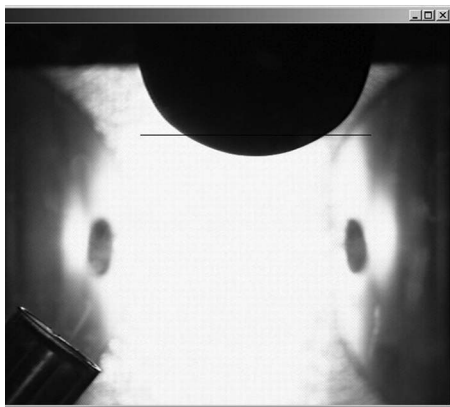

FIG. 3. Soot preform deposition.

FIG. 4. Image of the preform deposition region with the reference line positioned.
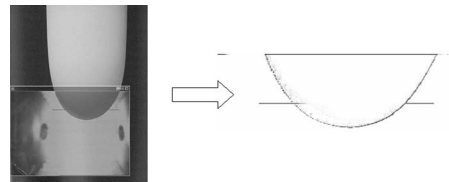

FIG. 5. Digital image processing for parametrization of the preform deposition surface profile.

trometer was used. Silica-germania samples were prepared by slicing consolidated preforms along their axes. The 3.0 mm thick disks were polished (optical finish) and the measurements were taken along their diameters in a 1.0 mm step.

IV. PARAMETRIZATION OF THE PREFORM DEPOSITION SURFACE PROFILE

To monitor the preform deposition surface profile, the deposition surface was parametrized through α and h parameters, where α is the power-law index profile that best fits the preform deposition surface profile, and h is the preform axial distance from the bottom tip to the reference diameter.

During the deposition stage, a CCD camera acquires the image of the preform bottom in real time. Over this digital image, a software treatment to obtain the preform deposition surface contour (Fig. 5) is performed. Afterwards, along this contour, various points were obtained, where the first point matches the preform tip lowest point, which was set to be the origin of the coordinate system. The preform deposition surface profile was parametrized by the following allometric function:[11]

$$y = cx^{\alpha}, \tag{1}$$

where y is the bottom height along the preform axis, c is a magnifying coefficient, x is the radial position, and α is the power-law index profile that best fits the preform deposition surface profile (Fig. 6).

Parametrization was carried out by considering points only in the right portion of the preform. Since the soot preform has a rotation movement during its deposition, it can be considered a revolution solid.
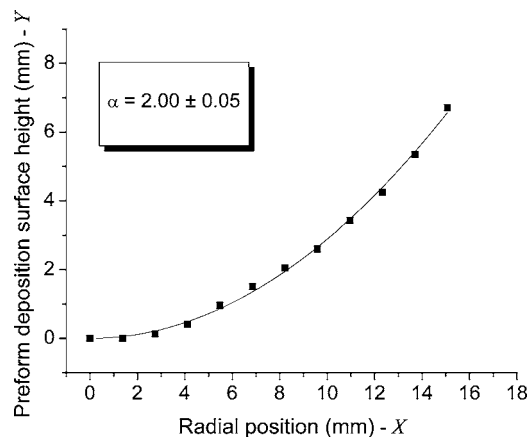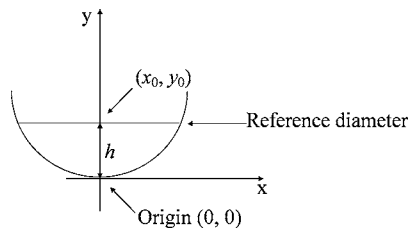
based on a standard personal computer (PC) was developed. This system acts automatically in the preform pulled up speed according to its growth rate, then maintains the preform diameter constant. Through an interface developed in National Instruments LABVIEW, one horizontal line (reference line) can be placed over the digital image of the preform bottom acquired by the charge coupled device (CCD) camera in real time. The reference line position on the preform image is fixed in relation to the burner exit and must be established at the beginning of each deposition according to the characteristics of the preform deposition region. Once the deposition region has the usual conical shape, there are parameters that determine the best position for the reference line.[15] Based on this horizontal line, the two points of the preform edge (one under the right edge and another under the left edge) are identified by image processing and the distance between them establishes a value for a reference diameter. Thus, this reference diameter is used in the automation process as a feedback for a Proportional-Integral-Derivative (PID) system in order to control the preform pull up speed, maintaining the uniformity of the porous preform diameter (Fig. 4).

After the deposition, the preforms were dehydrated for 2 h in a Cl_2 gas atmosphere at 1200 °C, followed by a consolidation for 2 h in He gas atmosphere at 1450 °C.

It is well known that the soot preform deposition and dehydration are basically the stages where the germanium doping profile formation of VAD preforms occurs. During the soot deposition, germania may be deposited as amorphous and/or crystalline phases according to the preform surface temperature that is established by many processing parameters.[10] The amorphous phase, which is formed in higher temperature regions, is very stable in the dehydration. On the other hand, the crystalline hexagonal phase, which is formed in lower temperature regions, is unstable for chlorination reaction in the dehydration process.[16] Previous experiments conducted in our laboratory showed that there are optimized processing conditions that maintain the germanium doping profile characteristics of unsintered soot preform related to the doping profile in the sintered preform.[10,17]

To determine the radial distribution of the germanium doping profile a Rigaku RIX3100 x-ray fluorescence spec-

FIG. 6. Parametrization of the soot preform deposition surface.

FIG. 7. *h* representation.

The *h* parameter was defined as the distance between the preform tip and the reference diameter mean point. The *h* value is obtained by the equation $h = y_0$, where y_0 is the ordinate of the reference diameter mean point on the preform axis (Fig. 7).

On the basis of a number of empirical data, a database was created correlating the α and *h* parameters to the corresponding doping profiles. Hence, a real time estimation of the refractive index profile was made possible.

V. STUDY OF THE REGION FOR A BETTER FITTING OF THE PREFORM DEPOSITION SURFACE PROFILE

For the development of an automation system, an effort was made in order to minimize the computational processing and establish a very fast system response with minimal performance impairments. A direct parametrization of the preform deposition surface profile through a nonlinear fitting would lead to an iterative method, which is not suitable for a real time processing. For this reason, the automation system applies a logarithmical function on the point coordinates and parametrizes the preform deposition surface through a linear fitting. However, the logarithmical function introduces some distortion in the parametrization when the deposition surface does not adjust the allometric function well.

In this way, instead of using many points to parametrize the entire preform deposition surface, regions of the preform bottom that best parametrize the whole preform deposition surface profile were studied, so that a small quantity of points can be used.

For a general case, several shapes of preform deposition surface were considered. More specifically, deposition surface profiles with parabolic ($\alpha = 1.97 \pm 0.02$), flat ($\alpha = 2.64 \pm 0.05$), and sharp ($\alpha = 1.35 \pm 0.03$) geometric shapes were studied (Fig. 8). In addition, preforms with suitable doping profiles, such as parabolic and triangular profiles, were also studied.

For each of these preforms, 12 points over the edges were obtained, in which the logarithmical function was applied, obtaining the linear function $Y = K + \alpha X$, where Y

FIG. 9. α values obtained by the derivative curve of function $Y = C + \alpha X$ of preforms with sharp, parabolic, and flat deposition surfaces.

$= \log y$, $k = \log c$, and $X = \log x$. The first derivative $Y'(X) = d(Y)/d(X)$ provides values for α, allowing one to find the best region for parametrization of preform deposition surface through its intersection with the $\alpha \pm 10\%$ (Figs. 9 and 10). This variation of 10% was obtained in previous studies and it represents the maximum variation of the α value during the deposition stage that does not significantly affect the germanium doping profile.[13]

Analyzing Fig. 9, it was possible to obtain radial intervals of soot preform bottoms which best parametrize the sharp, parabolic, and flat preform deposition surface profiles. The axial intervals were obtained applying the radial intervals in the allometric function (Table I).
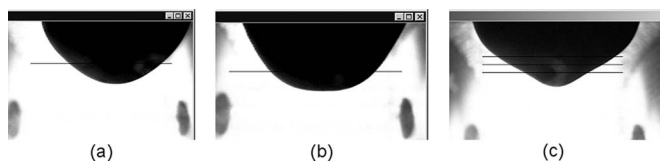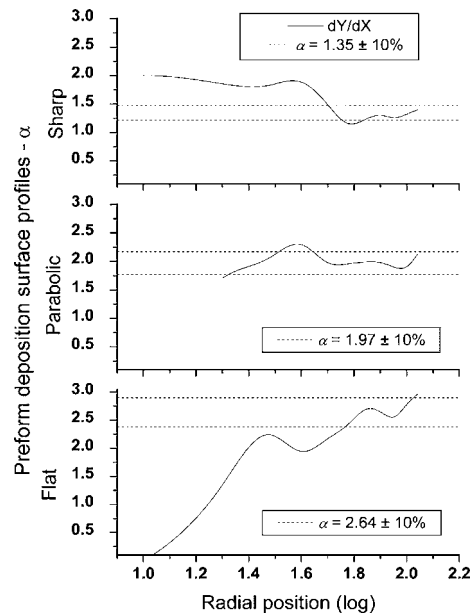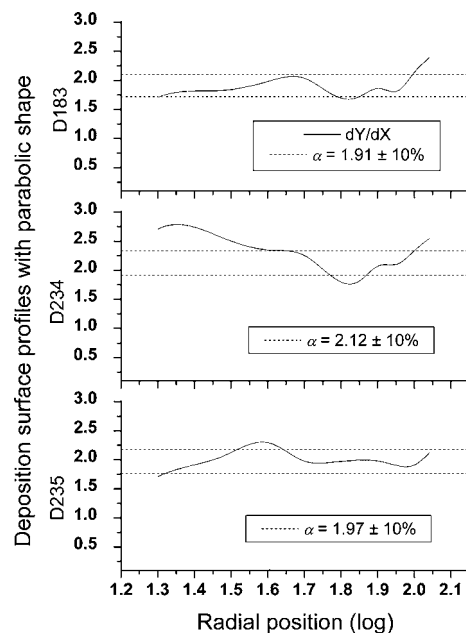

FIG. 8. Preform deposition surface profiles: (a) parabolic, (b) flat, and (c) sharp.

FIG. 10. α values obtained by the derivative curve of function $Y = C + \alpha X$ of preforms with parabolic and triangular doping profiles.

TABLE I. Best region for linear fitting for sharp, parabolic, and flat preform deposition surface profiles.

Preform	Deposition surface shape	Axial interval (mm)
D256	Sharp	[2.6, 3.1] or [4.1, 6.8]
D235	Parabolic	[0.3, 0.7] or [1.4, 7.1]
D216	Flat	[1.5, 7.8]

The same procedure was applied to preforms with parabolic and triangular doping profiles (Fig. 10 and Table II). Previous results showed that preform with parabolic doping profile can be achieved with a preform with $\alpha=2.0\pm0.2$ and $h=4.0\pm0.1$ mm. For triangular doping profile, $\alpha=2.0\pm0.2$ and $h=5.1\pm0.1$ mm.[13]

Also, it was noticed that sharp preform deposition surface profiles ($\alpha=1.35\pm0.03$ and $h=5.7\pm0.1$ mm) do not provide appropriate germanium doping profiles for optical fiber. Thus, preforms that present parabolic and triangular germanium doping profiles to determine the region that best parametrizes the preform deposition surface were considered. With the results from Figs. 9 and 10 and Tables I and II, it was concluded that the best region to be used for parametrization of the whole preform deposition surface is comprehended between 3.0 and 5.4 mm above the preform tip in the preform deposition surface.

Using points that belong to the 3.0–5.4 mm interval, the preform deposition surface profile was parametrized through the linear fittings (Fig. 11). From this figure and Fig. 8 it was noticed that the derivative curve of deposition surface profiles with parabolic shape is almost constant and practically remains in the $\alpha\pm10\%$ range. In these cases, almost all the points obey the $y=cx^\alpha$ function with accuracy, then when the logarithmical function in these points was applied, these ones continued to be aligned and the linear curve fits the points.

On the other hand, preforms with sharp and flat deposition surfaces are not so well parametrized by the allometric function. The derivative curve varies a lot and remains almost outside the range $\alpha\pm10\%$. In addition, the linearization by the logarithmical function gives rise to some distortion, mostly near the origin, due to particular features of this function. Once all points in the 3.0–5.4 mm interval are always aligned, it was concluded that three points in this interval are sufficient to parametrize the preform deposition surface profile through a linear fitting. Figure 12 shows the parametrization using the α values obtained from Fig. 11 by a linear curve fitting using three points belonging to the described interval.

The comparison among α values calculated by the nonlinear fitting using 12 points from the preform right edge

TABLE II. Best regions for a linear fitting of preforms with parabolic and triangular doping profiles.

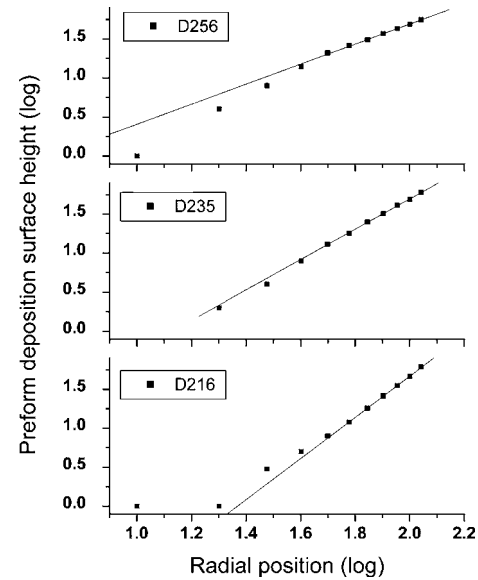| Preform	Doping profile	Axial interval (mm)
D183	Parabolic	$y=$[0.3, 2.2] or [2.9, 5.4]
D234	Parabolic	$y=$[1.1, 1.8] or [3.0, 5.6]
D235	Triangular	$y=$[0.3, 0.7] or [1.4, 7.1]

FIG. 11. From the top, linear curve fittings of a preform with sharp, parabolic, and flat deposition surfaces, respectively.

contour (Fig. 6) (α_{real}), α values obtained from Fig. 11 (α_{region}), and α values calculated by the linear fitting using 12 points from the preform right edge contour (α_{linear}) can be seen in Table III.

VI. DEVELOPMENT OF THE AUTOMATION SYSTEM FOR MONITORING THE PREFORM DEPOSITION SURFACE PROFILE

The automation system was developed using the National Instruments LABVIEW (Laboratory of Virtual Instrument Engineering Workbench) platform. LABVIEW is a powerful instrumentation and analysis software system for many architectures, including Macintosh Apple, Sun stations, and
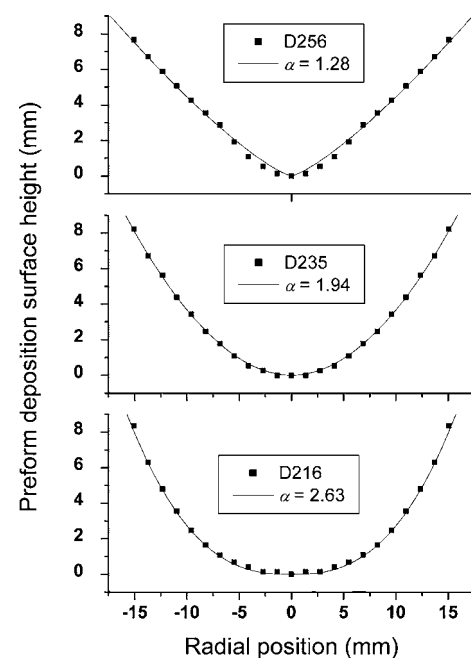

FIG. 12. Parametrization of preform deposition surface profile using α values obtained from the 3.0–5.4 mm region.

TABLE III. Accuracy improvement of α values calculated through the studied region.

Preform	α_{real}	α_{linear}	α_{region}
D256	1.35	1.65(22%)	1.28 (5%)
D235	1.97	2.02 (2%)	1.94 (1%)
D216	2.64	1.89(28%)	2.63(0.4%)

FIG. 13. Automation process and monitoring diagram of the preform deposition surface profile.

Microsoft Windows. Contrary to traditional programing languages, for example C/C++, LABVIEW features a graphical programing environment using block diagrams. LABVIEW can be used in many applications, including process control, automation, instrumentation, motion control, and simulation.[18,19]

In this way, to extend the automation system that controls the preform diameter uniformity, an automation system to estimate the germanium doping profile by monitoring the preform deposition surface profile during the deposition was developed in LABVIEW. The IMAQ VISION package was used for image acquisition and processing.

During the deposition stage, the image of the preform bottom is periodically acquired by a CCD camera and sent to a computer, where the system developed calculates the α and h distance values automatically. The α value is obtained using the preform origin point and three horizontal lines over the preform bottom. The origin coordinates are detected by the IMAQ Edge Tool, an IMAQ VISION tool component that uses three image parameters: contrast, width, and steepness. The contrast parameter specifies the threshold for the edge contrast. Only edges with a contrast greater than the specified value are used in the detection process. The width specifies the number of pixels that are averaged to find the contrast at each side of the edge. The steepness specifies the number of pixels that corresponds to the transition area of the image edge contrast using a line segment from the reference diameter mean point to image end. Under the junction of each one of the three horizontal lines and the preform right edge, three points are detected in the digital image, also by the IMAQ Edge Tool.

The software applies the logarithmic function over the points detected and a linear fitting is carried out through the following equation:

$$Y_i = k + \alpha X_i, \tag{2}$$

where $Y_i = \log y$ and $X_i = \log x$, for $i = 1, 2, 3$, which allows one to obtain the α value, where $\alpha = \log y / \log x$. The constant $k = 10^c$ is the linear coefficient.

The h distance is obtained by the difference between the reference diameter mean point and the preform origin (lowest point of preform deposition surface).

Figure 13 illustrates a diagram of automation system to control the *in situ* doping profile of VAD preform.

Calculating the α and h values with the accuracies of 5% and 3%, respectively, the LABVIEW platform showed its efficiency for the development of the automation system for the axial uniformity monitoring of the germanium doping profile during the deposition stage. The image in Fig. 14 illustrates its application for automation. In this image, the three hori-
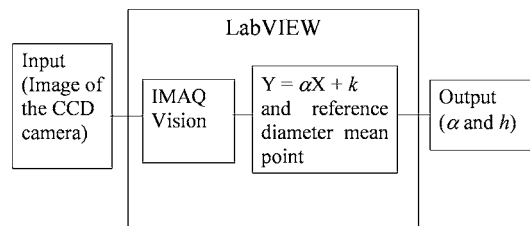
zontal lines and calculated α and h values are updated every 500 ms. The intermediary line was set to be the reference line, used as a feedback to the automated diameter control.

Knowing the values of α and h to obtain preforms with triangular and parabolic doping profiles,[13] the application of the automation system allowed one to establish the type of optical fiber to be produced, by reproducing the germanium doping profile of the preforms already conceived, and also identify the uniformity variation at the germanium doping profile along the preform axis.

VII. AXIAL UNIFORMITY OF GERMANIUM DOPING PROFILE

By using the automation system, it was possible to determine the maximum variation for both α and h parameters, in order to maintain the uniformity of the preform doping profile along its axial direction.

With a tight control of the deposition processing parameters, the D296 preform was produced with minimal variation in the α and h values, and a very small variation was also observed in the germanium doping profile (Fig. 15) which was measured in samples extracted from the upper and lower extremities of the preform. It was observed that both radial and axial distributions of germania concentrations remained uniform during the deposition. In this case, the maximum variations of 1.7% in the α value and 2.2% in the h value were not relevant to the uniformity of the germanium
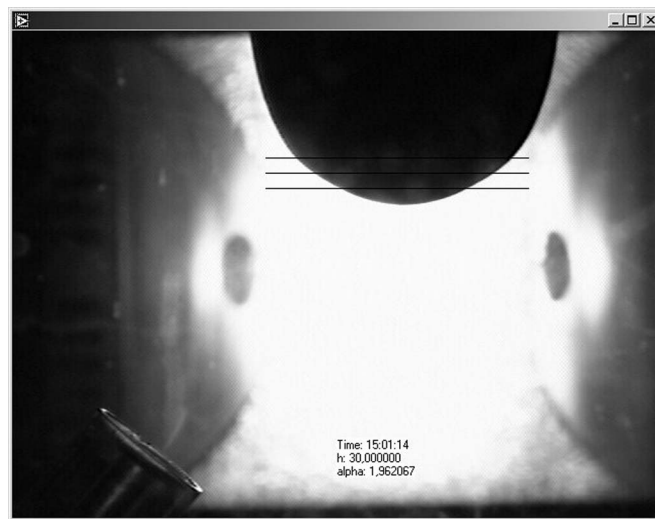

FIG. 14. Image of the preform deposition region after implementing the automation process to monitor the deposition surface profile.
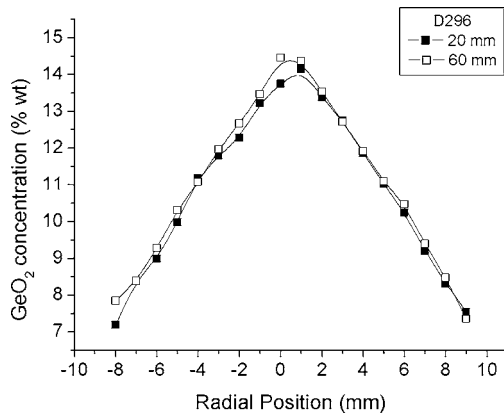
FIG. 15. Germanium doping profiles from the upper (60 mm) and lower (20 mm) extremities of the D296 preform after automation system implantation.

doping profile. For a general case, the doping profile will be axially uniform when the α and h parameter variations are smaller than 10.0% and 3.0%, respectively.[13]

On the other hand, for the D216 preform it was verified that the variations of 11.7% in the α value and 4.5% in the h value during the preform deposition changed significantly its germanium doping profile along the axial and radial directions. Figure 16 shows germanium doping profiles measured in samples obtained from both ends of the D216 preform (23 and 78 mm from the preform tip).

VIII. REPRODUCIBILITY OF PREFORM GERMANIUM DOPING PROFILE

The reproducibility of the germanium doping profile is an essential element to make a mass production of optical fiber preforms viable. The implantation of the automation system corroborated the possibility of obtaining a high reproducibility of the germanium doping profile. For D183 (α =1.91±0.04 and h=3.9±0.1 mm) and D234 (α=2.12±0.05 and h=3.9±0.1 mm) preforms, produced under the same deposition conditions, it was verified that both preforms showed similar parabolic shape germanium doping profiles (Fig. 17). By changing processing parameters, the D250 (α =1.96±0.02 and h=4.4±0.1 mm) and D251 (α=1.97±0.01
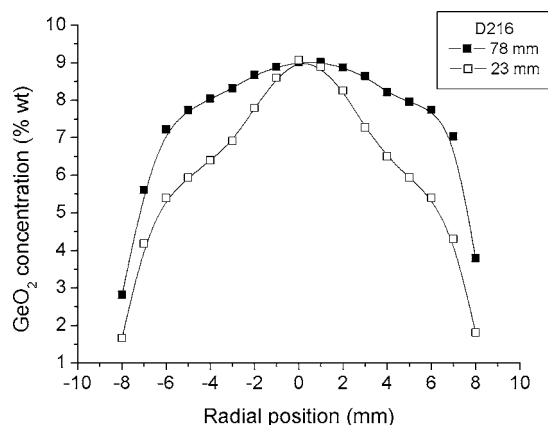

FIG. 16. Germanium doping profiles from the upper (78 mm) and lower (23 mm) extremities of the D216 preform with great variation in the α and h parameters.
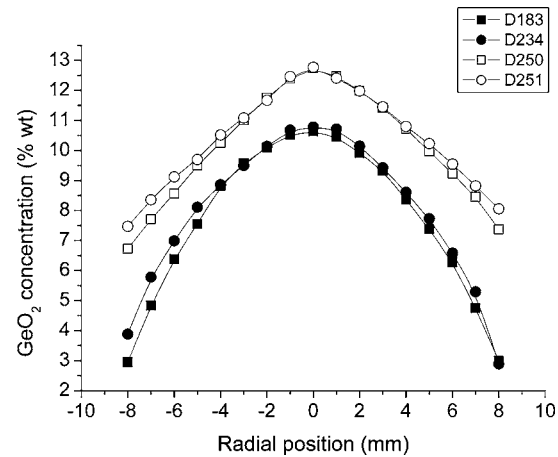

FIG. 17. Germanium doping profiles of preforms D183 (α=1.91±0.04 and h=3.9±0.1 mm), D234 (α=2.12±0.05 and h=3.9±0.1 mm), D250 (α =1.96±0.02 and h=4.4±0.1 mm), and D251 (α=1.97±0.01 and h =4.7±0.1 mm).

and h=4.7±0.1 mm) preforms, deposited under the same conditions, showed similar triangular shape germanium doping profiles (Fig. 17). In general, it was verified that the reproducibility of germanium doping profiles is possible when the maximum variations of α and h values among preforms are 10.0% and 3.0%, respectively.[13]

IX. DISCUSSION

The automation system developed in LABVIEW showed to be very effective for monitoring and parametrization of the preform deposition surface profile during the deposition stage. This system made possible to estimate the germanium doping profiles and, consequently, the refractive index profiles of VAD preforms. It was verified that, for preforms obtained in the present research, only three points located in the preform deposition surface between 3.0 and 5.4 mm above the preform tip are sufficient to parametrize the whole preform deposition surface profile, providing a very fast system response with a minimal computational processing and a quite good precision of 2.0%.

By monitoring the preform deposition surface and calculating the corresponding α and h parameters, the system made it possible to reproduce a desired germanium doping profile as well as to monitor its axial uniformity in real time. For both cases, the maximum allowed variations of α and h parameters during the deposition were determined to be up to 10% and 3%, respectively. Immediate contribution is the reduction of preform rejects and great improvement of production cost as well as for research and development of special fibers. Moreover, through a database of processing parameters that correlates the α and h parameters and the corresponding doping profiles, it is possible to produce preforms with a predetermined refractive index profile by adjusting the processing parameters at the beginning of each preform deposition.

ACKNOWLEDGMENTS

[1] A. M. Glass, D. J. DiGiovani, T. A. Strasser, A. J. Stentz, R. E. Slusher, A. E. White, A. R. Kortan, and B. J. Eggleton, Bell Labs Tech. J **5**, 168 (2000).
[2] H. Shimizu, D. Torikai, and C. K. Suzuki, Proceedings of the First Workshop on QITS: Materials Life-Cycle and Sustainable Development, Campinas, SP, Brazil (The United Nations University, Institute of Advanced Studies, Tokyo, 1998), Vol. 1, p. 79.
[3] K. Sanada, T. Shiota, and K. Inada, J. Non-Cryst. Solids **188**, 275 (1995).
[4] P. Nouchi, L. A. Montmorillon, P. Sillard, A. Bertaina, and P. Guenot, C. R. Phys. **4**, 29 (2003).
[5] Y. Y. Huang, A. Sarkar, and J. Schultz, J. Non-Cryst. Solids **27**, 29 (1977).
[6] J. W. Fleming, Appl. Opt. **23**, 4486 (1984).
[7] T. Izawa, IEEE J. Sel. Top. Quantum Electron. **6**, 1220 (2000).
[8] T. Izawa and S. Sudo, in *Optical Fibers: Material and Fabrication*, edited by KTK Scientific (Kluwer Academic Publishers Group, Tokyo, 1987), p. 123.
[9] T. Edahiro, M. Kawachi, S. Sudo, and S. Tomaru, J. Appl. Phys. **19**, 2047 (1980).
[10] E. H. Sekiya, D. Torikai, E. Gusken, D. Y. Ogata, R. F. Cuevas, and C. K. Suzuki, J. Non-Cryst. Solids **273**, 228 (2000).
[11] K. Imoto, M. Sumi, and T. Suganuma, J. Lightwave Technol. **6**, 1376 (1988).
[12] K. Chida, H. Yokota, M. Kyoto, H. Sato, M. Watanabe, and N. Yoshiota, U.S. Patent No. 4,797,143, (January 10, 1989).
[13] J. S. Santos, E. Ono, E. Gusken, and C. K. Suzuki, J. Lightwave Technol. **24**, 831 (2006).
[14] K. Chida, M. Nakahara, S. Sudo, and N. Inagaki, J. Lightwave Technol. **LT-1**, 56 (1983).
[15] C. K. Suzuki, D. Torikai, E. H. Sekiya, and E. Ono, patent requested from the INPI, Brazil, protocol No. PI0203755–6, 2002.
[16] K. Sanada, T. Moriyama, and K. Inada, J. Non-Cryst. Solids **194**, 163 (1996).
[17] R. F. Cuevas, E. Gusken, E. H. Sekiya, D. Y. Ogata, D. Torikai, and C. K. Suzuki, J. Non-Cryst. Solids **273**, 252 (2000).
[18] R. Jamal, Nucl. Instrum. Methods Phys. Res. A **352**, 438 (1994).
[19] H. A. Andrade and S. Kovner, Conference Record of the Thirty-Second Asilomar Conference on Signals, Systems & Computers IEEE Conference Proceedings, Pacific Grove, California, vol. **2**(1-4), pp. 1705–1709 (1998).